Fiber Optofluidic Microlaser With Lateral Single Mode Emission

Chao-Yang Gong, Yuan Gong, Wei-Li Zhang, Yu Wu, Yun-Jiang Rao, *Fellow, IEEE*, Gang-Ding Peng, and Xudong Fan

***Abstract*—We report a low threshold fiber optofluidic microlaser, based on a microstructured optical fiber (MOF). The particular MOF structure is used not only as the microfluidic channel for sampling the liquid gain, but also as a spectral filter to achieve the single mode emission. Lateral laser emission from the MOF is observed when 1 mM Rhodamine 6G in ethanol is sucked into the MOF by the capillary force and pumped with a pulsed laser. It requires a low volume, $\sim$470 pL, of the gain materials. Single mode emission with a full width at half-maximum (FWHM) of 53 pm is obtained with a threshold of 13.2 μJ/mm^2. The filtering effect is investigated both experimentally and theoretically by the interference within the cavity. The dependence of the number of modes on the lateral position of the pump with respect to the MOF is also discussed By using the single mode emission, it is promising for the multiplexing of optofluidic lasers in the spectral domain.**

***Index Terms*—Optofluidic laser, microstructured optical fiber (MOF), single mode emission.**

I. Introduction

OPTOFLUIDIC laser is an emerging technology that integrates micro laser cavity with liquid gain medium. It has been developed to be a powerful tool for biochemical detection because of the enhanced sensitivity with the laser cavity [1], [2]. However, most of the optofluidic lasers are multimode using laser cavities, such as ring resonator [3]–[13], micro beads [14] and liquid droplet [15]. Comparing with the multimode emission, the advantages of using single mode lasers for sensing are threefold. First, for the intensity-based interrogation, the output of the single mode laser has potentially higher stability than the multimode laser, due to the absence of the mode competition [16]–[18]. Second, single mode emission makes available the spectral interrogation by the detection of wavelength shift [27], which is difficult for the multimode lasers when the shift is larger than the mode spacing. Usually, the spectral interrogation offers higher sensitivity than using the intensity-based interrogation. Third, the capability of wavelength multiplexing for single mode lasers is inherently better than the multimode lasers, as the linewidth of the single mode emission is much narrower than the multimode. Importantly, by wavelength multiplexing [19]–[24], an array of single mode lasers can be developed for high throughput detection of biochemical analyte. It is worth noting that the wavelength multiplexing of single mode optofluidic lasers remains unexplored due to the lack of proper lasers.

There were mainly two strategies for developing single mode lasers. One is by using a tiny laser cavity with very short cavity length, letting only one longitudinal mode fell into the gain band of the laser material [25]. This method has strict requirement on the gain medium, such as broad gain bandwidth, high efficiency of slope efficiency. The other is by using different filtering effects to achieve the single mode lasing [26]–[37]. A coupled ring resonator, by employing the Vernier effect between two ring resonators, was developed by Wu et al. to generate a single mode laser. The emission was strongly dependent on the coupling coefficient between the two resonators [26]–[30]. Other schemes required special designs of on-chip filters by using distributed feedback structures or Bragg gratings [31]–[37], which require expensive fabrication facility and complicated process.

Here, we proposed and demonstrated a novel single mode optofluidic laser by employing microstructured optical fiber (MOF) as both the microfluidic channel and the intra-cavity filter. Inherently different from the traditional fiber lasers which employ the waveguiding core of optical fibers and prefer an all-fiber structure, the proposed fiber optofluidic laser used the cross-section of a MOF for spectral filtering and sampling. The fiber was sandwiched between two reflective mirrors, forming a Fabry-Perot (FP) cavity and providing the optical feedback, as shown in Fig. 1(a). In the cross-section, the MOF has two air holes (Fig. 1(b)) that can serve as the channels for sampling the liquid gain material, i.e., Rhodamine 6G (R6G) in ethanol. Under lateral pumping by a pulsed laser, single mode lasing was achieved when the two holes were aligned along the axis of the FP cavity and the beam position of pump laser was optimized. This method for single mode lasing is simple, stable and the

Manuscript received April 17, 2017; revised May 17, 2017; accepted June 1, 2017. This work was supported in part by the National Natural Science Foundation of China under Grant 61575039, in part by the Fundamental Research Funds for the Central Universities under Grant ZYGX2015J137, and in part by the 111 Project under Grant B14039. *(Corresponding author: Yuan Gong.)*

C.-Y. Gong, W.-L. Zhang, Y. Wu, and Y.-J. Rao are with the Key Laboratory of Optical Fiber Sensing and Communications (Ministry of Education), University of Electronic Science and Technology of China, Chengdu 611731, China (e-mail: gongcyde@std.uestc.edu.cn; wl_zhang@uestc.edu.cn; wuyuzju@163.com; yjrao@uestc.edu.cn).

Y. Gong is with the Key Laboratory of Optical Fiber Sensing and Communications (Ministry of Education), Center for Information in BioMedicine, University of Electronic Science and Technology of China, Chengdu 611731, China and Department of Biomedical Engineering, University of Michigan, Ann Arbor, MI 48109 USA (e-mail: ygong@uestc.edu.cn).

G.-D. Peng is with the School of Electrical Engineering and Telecommunications, University of New South Wales, Sydney, NSW 2052, Australia (e-mail: g.peng@unsw.edu.au).

X. Fan is with the Department of Biomedical Engineering, University of Michigan, Ann Arbor, MI 48109 USA (e-mail: xsfan@umich.edu).

Color versions of one or more of the figures in this paper are available online at http://ieeexplore.ieee.org.

Digital Object Identifier 10.1109/JSTQE.2017.2712622

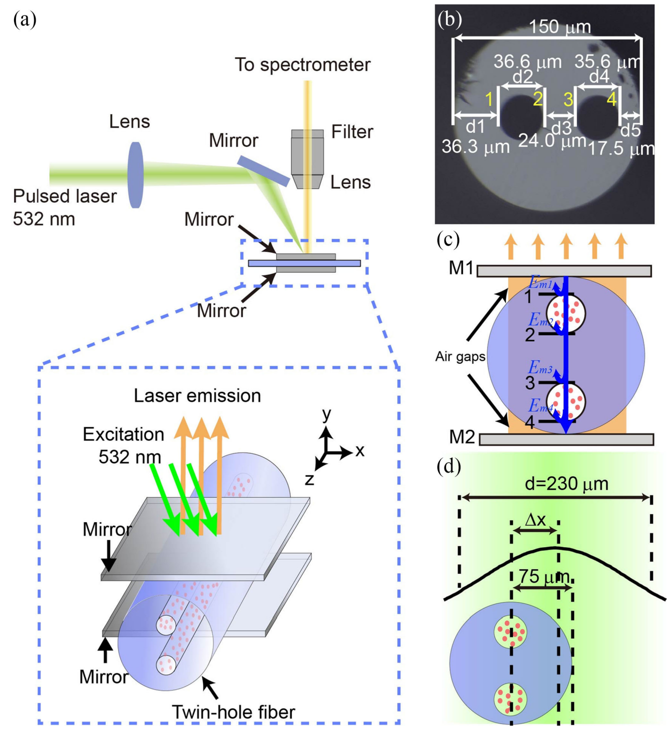

Fig. 1. (a) Schematic diagram of the experimental setup. Inset, an enlargement of the fiber optofluidic laser. (b) Microscope image of the cross-section of the microstructured optical fiber. (c) Illustration of the intra-cavity filtering effect. (d) The relative position between the pump laser beam and the MOF.

directional emission is easy to collect. The open holes of the MOF provide sampling channels to include biochemical reactions into the laser cavity, which is promising for biochemical detection like enzyme linked immunosorbent assay (ELISA) [38].

II. Experimental Setup

Fig. 1(a) shows the schematic diagram of the fiber optofluidic laser. The MOF was sandwiched between two mirrors with reflectivities of 91.5% (upper) and 99.5% (bottom), respectively. Another fiber with the same diameter as the MOF was used as a support to keep the mirrors in parallel. The geometry of the MOF is shown in Fig. 1(b). The MOF of 150 μm outer diameter has two air holes of $\sim$36 μm diameter. As shown in Fig. 1(c), the orientation of the MOF was adjusted such that the two holes are aligned along the cavity and acted as cascaded in-cavity filters.

Thanks to the capillary force, the gain medium of 1 mM R6G in ethanol was easily sucked into the MOF through the two holes. A 532 nm pulsed laser (Contiuum, 5 ns pulse width, 20 Hz repetition rate) was used as the pump and focused on the MOF through the upper mirror at an angle of 15°. The pump energy was monitored by an energy meter. The diameter of the pump beam on the MOF was about 230 μm, by which the pump energy density can be calculated. Once the gain medium was excited, the light was reflected back and forth in the cavity and amplified. The lateral laser emission was collected by a lens and sent to the spectrometer (Andor, SR-500I-A). A long-pass filter with a cutoff wavelength of 550 nm was used to filter out the pump laser. The influence of the beam position of the pump laser on the optofluidic laser was investigated by laterally adjusting the MOF step-by-step along the x axis, with a step size of 5 μm (Fig. 1(d)).

The motivation of using the MOF is threefold. First, thanks to its curved shape, the MOF can act as a micro lens in the parallel FP cavity in order to reduce the propagation loss of light in the cavity, especially after multiple reflections. Second, the holes of MOF act as natural microfluidic channels for sampling. As the diameter of the holes is in tens of micrometers, the capillary force is strong enough for sucking the liquid gain into the MOF efficiently. The MOF microfluidic channel requires a low volume of 470 pL for the gain material. Third, the MOF serves as an intra-cavity filter, making available the single mode laser emission, which will be discussed in detail in the next section.

III. Theoretical Model

We develop a theoretical model to analyze the filtering effect of the MOF. Especially, the interference among the weak reflections from the surfaces of holes is considered, since the strong interference between the cavity mirrors only leads to uniform comb of fringes. The electric field of light reflected from interface p ($p = 1, 2, 3, 4$) in the 0th roundtrip can be written as

$$E_{0p} = E_0 r_p \left(\prod_{j=1}^{p} t_{j-1}^2 \right) \exp\left(-ik2 \sum_{j=1}^{p} n_j d_j \right) \qquad (1)$$

Here, E_0 is the initial electric field on the inner surface of M_1. r_p, t_p are the amplitude reflection and transmission coefficients of interface p (Fig. 1(c)). t_0 equals unity. $k = 2\pi/\lambda$ is the wave number with λ the wavelength. d_j ($j = 1, 2, 3, 4, 5$) are the geometric parameters (Fig. 1(b)) and n_j is the corresponding refractive index of the silica and the liquid. In the mth roundtrip, the electric field can be expressed as

$$E_{mp} = E_{0p} A^m. \qquad (2)$$

Here, A is a roundtrip coefficient including both amplitude and phase changes, giving by

$$A = r_{M_1} r_{M_2} \left(\prod_{j=1}^{4} t_j^2 \right) \exp\left(-i2k \sum_{j=1}^{5} n_j d_j \right) \qquad (3)$$

Here, r_{M_1}, r_{M_2} are the amplitude reflection coefficients of M_1 and M_2, respectively. The electric field of all the reflections from the interfaces can be summed up to be

$$B = \sum_{m=0}^{N_1} \sum_{p=1}^{4} E_{mp}. \qquad (4)$$

Here, N_1 denotes how many times the light travels along the axis of cavity, which can be reflected on the interfaces.

Considering each reflection term in (4) as a new source, the light can be reflected by the mirrors for several times and will gradually propagate off the axis. In N_2 roundtrips, it can still be collected by the spectrometer before finally escaping from

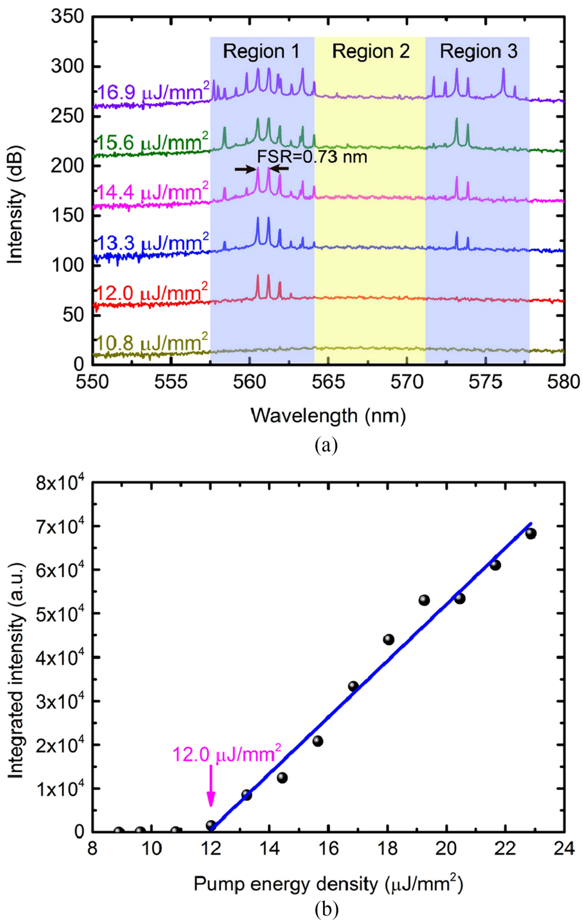

Fig. 2. (a) Normalized emission spectra at different pump energy density. (b) The spectrally integrated intensity as a function of pump energy density. The intensity is integrated between 557 nm and 577 nm.

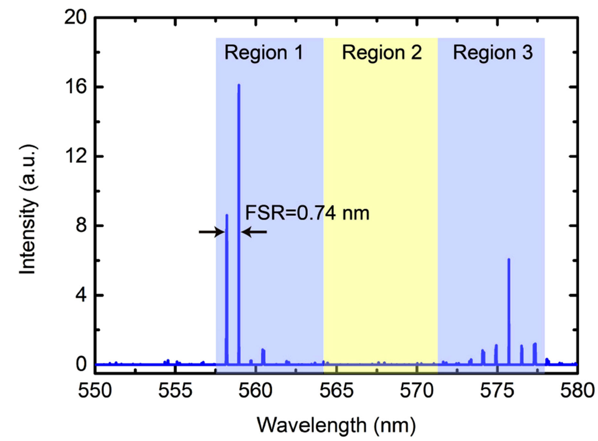

Fig. 3. The simulated interference spectrum.

the laser cavity. Therefore, the interference occurs among all the beams travelling either on-axis or off-axis. The total sum of electric fields is given by

$$E = t_{M_1} B \sum_{n=0}^{N_2} A^n \exp\left(-ink\Delta D\right). \tag{5}$$

Here, t_{M_1} is the transmission coefficient of M_1. ΔD is an additional optical path difference related to the air gaps (Fig. 1(c)) and is negative as the index of air is lower than that of silica. Finally, the filtering function for the MOF can be defined as

$$F(\lambda) = \frac{E(\lambda)\, E^*(\lambda)}{E_0 E_0^*}. \tag{6}$$

Based on the filtering function, the simulation results are given and discussed in the next section.

IV. Results and Discussion

Firstly, the position of the MOF was optimized to maximize the laser output, which we defined as $\Delta x = 0$. In this case, no single mode emission was observed. Fig. 2(a) shows the normalized laser spectra in logarithmic scale under different pump energy density, which was estimated by the pump energy and the pump beam radius on the MOF. The free spectral range (FSR) was 0.73 nm. With an increasing pump energy density, more longitudinal modes were observed. Fig. 2(b) shows the spectrally integrated intensity as a function of the pump energy density, showing a threshold of 12.0 μJ/mm^2. Comparing with the previous fiber optofluidic laser [9], [10], [39], the low threshold was due to the high quantum yield of R6G and relative low loss of the MOF-incorporated FP cavity with a short cavity length of 150 μm.

The laser peaks in Fig. 2(a) appeared only in two separate regions (region 1 and region 3). No laser emission was observed in region 2, which is different from the conventional optofluidic laser based on microring or Fabry-Perot resonators [3]–[15]. The strong suppression of laser modes in region 2 is due to the filtering effect caused by the twin-hole structure of the MOF.

The interference in the cavity was discussed in Section III. Based on the theoretical model, the interference spectrum was numerically simulated and shown in Fig. 3. In the simulation, d_i ($i = 1, 2, 3, 4, 5$) was set according to the structure parameters shown in Fig. 1(b). The refractive index were set as $n_1 = n_3 = n_5 = 1.45$ and $n_2 = n_4 = 1.36$. The additional optical path, $\Delta D = 19$ μm, was used by considering the gas gap between the fiber and the mirrors. $r_{M_1}^2 = 0.91$, $r_{M_2}^2 = 0.99$ and $N_1 = N_2 = 100$ was used in the simulation. The simulated spectrum shows a filtering effect, similar to the experimental spectra, that laser modes in region 2 are suppressed. The corresponding FSR in the simulated spectra is 0.74 nm, which is almost equal to the FSR obtained in Fig. 2(a). The difference between the simulation and the experimental observation is due to the slight changes of the diameter of the MOF during its being sandwiched in the FP cavity. With the amplification of laser cavity with gain, the filtering effect can be further strengthened.

Secondly, single mode laser was demonstrated by adjusting the lateral displacement between the MOF and the pump beam, denoting by Δx in Fig. 1(d). The MOF was laterally moved with a step size of 5 μm. The pump energy density was fixed at 14.4 μJ/ mm^2. The diameter of the pump beam on the MOF was 230 μm, about 6 times larger than the size of the inner holes. The emission spectra with different Δx are plotted in Fig. 4(a). In order to further illustrate the evolution of the modes, we

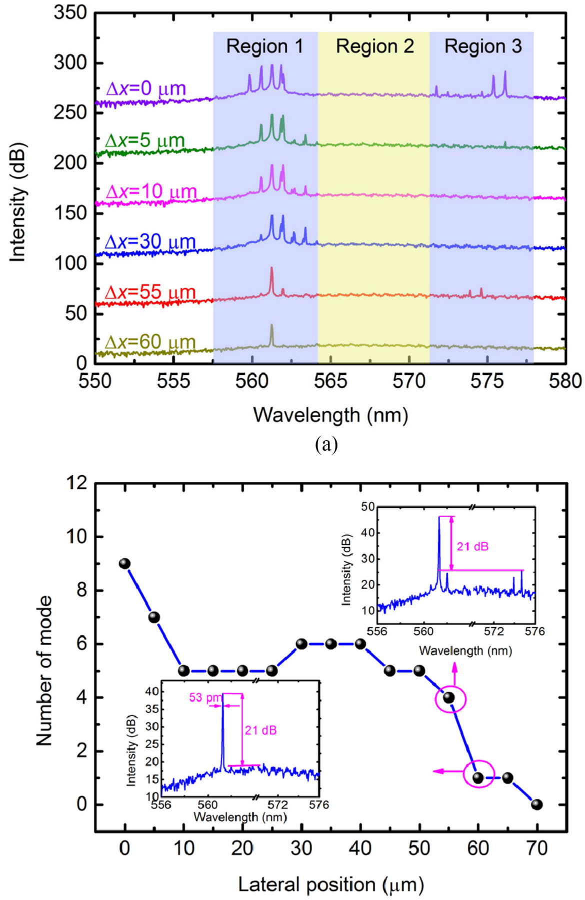

Fig. 4. (a) The laser spectra with different lateral displacement of the pump beam. (b) Number of modes as a function of Δx.

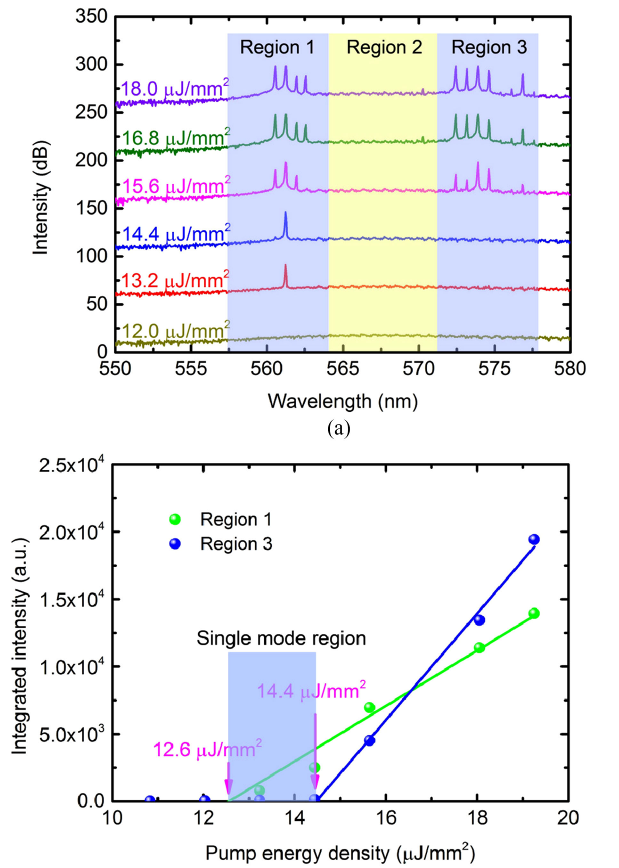

Fig. 5. (a) The normalized laser spectrum at various pump energy density. (b) The integrated intensity as a function of the pump energy density.

defined the peaks where the signal to noise ratio (SNR) exceeds 5 dB as a mode. The number of modes was counted in each spectrum and plotted as a function of Δx in Fig. 4(b). Initially, with $\Delta x = 0$, the laser modes appeared in both regions 1 and 3. With an increasing Δx, the modes in region 3 disappeared and the number of modes in region 1 continued to decrease. Finally, a single mode lasing at 561.2 nm was obtained with Δx of between 60 μm and 65 μm. The fluctuation of number of modes between $\Delta x = 10$ μm and $\Delta x = 55$ μm might be caused by the mode competition. The '0' modes indicate no laser emission was observed. By offset aligning the pump laser, ΔD (the air gap) increases and the filtering function of MOF also changes, enabling the single mode lasing. The bottom left inset of Fig. 4(b) shows the spectrum of the single mode laser with an offset of $\Delta x = 60$ μm, showing a narrow full width at half maximum (FWHM) of 53 pm. A SNR of 21 dB is obtained, which is comparable to that of the single mode lasing based on the coupled ring resonators (19.6 dB, [30]). With an offset of $\Delta x = 55$ μm, the best side mode suppression ratio (SMSR) was also 21 dB, as shown in the upper right inset of Fig. 4(b).

Thirdly, by fixing at $\Delta x = 60$ μm, the laser spectra were recorded at different pump energy density, as shown in Fig. 5(a). Single mode laser was observed when pump energy density is between 13.2 μJ/mm^2 and 14.4 μJ/mm^2. When further increasing the energy density, the multimode lasing occurred. The modes were fallen into two bands in the spectra, similar to the results in Fig. 2. Fig. 5(b) shows the lasing threshold of 12.6 μJ/mm^2 and 14.4 μJ/mm^2, for region 1 and region 3, respectively. The intensity was spectrally integrated between 559 nm $\sim$ 563 nm, 570 nm $\sim$ 580 nm, respectively. The threshold for region 1 is lower than that of region 3, making it available to select a single mode for lasing between the threshold difference. The threshold values for region 1 and 3 are different due partially to the destructive interference from MOF. Another factor is that the maximum gain of R6G is closer to region 1 than region 3.

The three regions in the laser spectra were roughly defined in this paper. The full spectral width of the fiber optofluidic laser is dominated by the gain spectra of R6G and the pump energy density. Experimental results in Figs. 2(a) and 5(a) show that the laser modes in regions 1 and 3 increases when the pump energy density increases. On the other hand, the extinction of modes in region 2 is resulted from the destructive interference among beams reflected from the cavity and the MOF.

At last, as a control experiment, we replaced the fiber with a round silica capillary. The commercial capillary (VitroCom 1017Q) with an outer diameter (OD) of 170 μm and inner diameter (ID) of 100 μm was sandwiched between the same mirrors as described previously. The gain material and the pump were

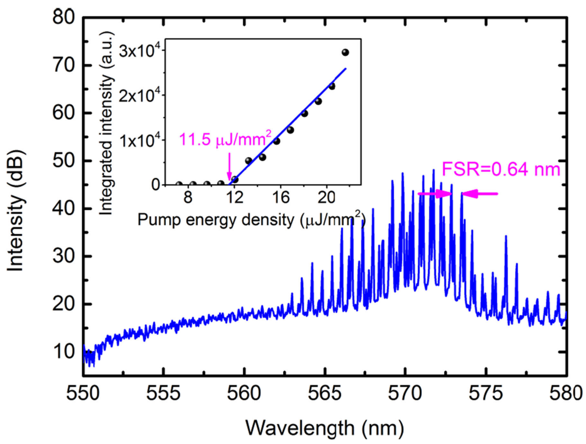

Fig. 6. The laser spectrum by using a round capillary instead of the MOF. Pump energy density was fixed at 12.0 μJ/mm^2, which was slightly above the threshold. Inset, the intensity as a function of pump energy density, showing a threshold of 11.5 μJ/mm^2.

also the same. The twin-hole fiber and the capillary are similar in size, but different in the cross-section. Fig. 6 shows the emission spectrum with a pump energy density of 12.0 μJ/mm^2. The FSR of the emission spectrum was about 0.64 nm, agreeing well with that calculated from the OD of the capillary. There was a redshift of about 5 nm of the laser spectrum, due to the higher absorption caused by the relatively larger volume of gain medium in the capillary than in the MOF. The threshold of the capillary-based optofluidic laser was about 11.5 μJ/mm^2, as shown in the inset. Although the pump energy density was only slightly above the threshold, a clear multimode feature was observed. No single mode lasing can be obtained with the capillary, indicating that the filtering effect of the MOF is necessary and crucial for the single mode optofluidic laser.

V. Conclusion

We have demonstrated a fiber optofluidic laser with lateral single mode emission, based on a MOF with two holes that acts as both the microfluidic channels and the filtering elements. Thanks to the unique structure of the microstructured optical fiber, single mode laser was achieved with a SNR of 21 dB by adjusting the displacement of the pump beam. The threshold of the single mode lasing is about 13.2 μJ/mm^2 and the linewidth can be as narrow as 53 pm. The narrow linewidth is promising for the wavelength multiplexing applications using an array of the optofluidic lasers.

References

[1] X. Fan and S. H. Yun, "The potential of optofluidic biolasers," *Nature Methods*, vol. 11, pp. 141–147, Feb. 2014.

[2] M. Aas, Q. Chen, A. Jonáš, A. Kiraz, and X. Fan, "Optofluidic FRET lasers and their applications in novel photonic devices and biochemical sensing," *IEEE J. Sel. Topics Quantum Electron.*, vol. 22, Jul. 2016, Art. no. 7000215.

[3] Y. Sun, S. I. Shopova, C. S. Wu, S. Arnold, and X. Fan, "Bioinspired optofluidic FRET lasers via DNA scaffolds," *Proc. Natl. Acad. Sci. U.S.A.*, vol. 107, pp. 16039–16042, Sep. 2010.

[4] X. Zhang *et al.*, "Coupled optofluidic ring laser for ultrahigh-sensitive sensing," *Opt. Express*, vol. 19, pp. 22242–22247, Oct. 2011.

[5] X. Zhang, W. Lee, and X. Fan, "Bio-switchable optofluidic lasers based on DNA Holliday junctions," *Lab Chip*, vol. 12, pp. 3673–3675, Jul. 2012.

[6] Q. Chen *et al.*, "Highly sensitive fluorescent protein FRET detection using optofluidic lasers," *Lab Chip*, vol. 13, pp. 2679–2681, Mar. 2013.

[7] Q. Chen, A. Kiraz, and X. Fan, "Optofluidic FRET lasers using aqueous quantum dots as donors," *Lab Chip*, vol. 16, pp. 353–359, Jan. 2016.

[8] Y. C. Chen, Q. Chen, and X. Fan, "Optofluidic chlorophyll lasers," *Lab Chip*, vol. 16, pp. 2228–2235, May 2016.

[9] Q. Chen, M. Ritt, S. Sivaramakrishnan, Y. Sun, and X. Fan, "Optofluidic lasers with a single molecular layer of gain," *Lab Chip*, vol. 14, pp. 4590–4595, Dec. 2014.

[10] W. Lee, Q. Chen, X. Fan, and D. K. Yoon, "Digital DNA detection based on a compact optofluidic laser with ultra-low sample consumption," *Lab Chip*, vol. 16, pp. 4770–4776, Nov. 2016.

[11] Y. C. Chen, Q. Chen, and X. Fan, "Lasing in blood," *Optica*, vol. 3, pp. 809–815, Jul. 2016.

[12] Q. Chen *et al.*, "Self-assembled DNA tetrahedral optofluidic lasers with precise and tunable gain control," *Lab Chip*, vol. 24, pp. 3351–3354, Jun. 2013.

[13] Z. L. Li *et al.*, "A simplified hollow-core microstructured optical fibre laser with microring resonators and strong radial emission," *Appl. Phys. Lett.*, vol. 105, Aug. 2014, Art. no. 071902.

[14] M. Humar and S. H. Yun, "Intracellular microlasers," *Nature Photon.*, vol. 9, pp. 572–576, Sep. 2015.

[15] S. K. Y. Tang *et al.*, "A multi-color fast-switching microfluidic droplet dye laser," *Lab Chip*, vol. 9, pp. 2767–2771, Aug. 2009.

[16] L. M. Narducci and J. R. Tredicce, "Mode-mode competition and unstable behavior in a homogeneously broadened ring laser," *Phys. Rev. A*, vol. 33, pp. 1842–1854, Mar. 1986.

[17] S. Singh and L. Mandel, "Mode competition in a homogeneously broadened ring laser," *Phys. Rev. A*, vol. 20, p. 2459–2463, Dec. 1979.

[18] J. Dong and K. I. Ueda, "Longitudinal-mode competition induced instabilities of Cr4+, Nd3+: Y3Al5O12 self-Q-switched two-mode laser," *Appl. Phys. Lett.*, vol. 87, Oct. 2005, Art. no. 151102.

[19] E. Petryayeva and W. R. Algar, "Multiplexed homogeneous assays of proteolytic activity using a smartphone and quantum dots," *Anal. Chem.*, vol. 86, pp. 3195–3202, Feb. 2014.

[20] W. Zhou, W. Liang, D. Li, R. Yuan, and Y. Xiang, "Dual-color encoded DNAzyme nanostructures for multiplexed detection of intracellular metal ions in living cells," *Biosens. Bioelectron.*, vol. 85, pp. 573–579, May 2016.

[21] I. C. Wu *et al.*, "Squaraine-based polymer dots with narrow, bright near-infrared fluorescence for biological applications," *J. Amer. Chem. Soc.*, vol. 137, pp. 173–178, Dec. 2014.

[22] S. Spindel, J. Balsam, G. Mattay, and K. E. Sapsford, "Investigating low volume planar surface fluorescent immunoassays with QDs for spatial and spectral multiplexing," *Sens. Actuators, B*, vol. 215, pp. 396–404, Apr. 2015.

[23] R. Hu *et al.*, "Multicolor fluorescent biosensor for multiplexed detection of DNA," *Anal. Chem.*, vol. 86, pp. 5009–5016, Apr. 2014.

[24] M. Han, X. Gao, J. Z. Su, and S. Nie, "Quantum-dot-tagged microbeads for multiplexed optical coding of biomolecules," *Nature Biotechnol.*, vol. 19, pp. 631–635, Jul. 2001.

[25] W. Wang *et al.*, "Optofluidic laser array based on stable high-Q Fabry–Pérot microcavities," *Lab Chip*, vol. 15, pp. 3862–3869, Aug. 2015.

[26] W. Lee *et al.*, "Tunable single mode lasing from an on-chip optofluidic ring resonator laser," *Appl. Phys. Lett.*, vol. 98, Feb. 2011, Art. no. 061103.

[27] X. Wu, Y. Sun, J. D. Sutter, and X. Fan, "Single mode coupled optofluidic ring resonator dye lasers," *Appl. Phys. Lett.*, vol. 94, Jun. 2009, Art. no. 241109.

[28] H. Li, L. Shang, X. Tu, L. Liu, and L. Xu, "Coupling variation induced ultrasensitive label-free biosensing by using single mode coupled microcavity laser," *J. Amer. Chem. Soc.*, vol. 131, pp. 16612–16613, Nov. 2009.

[29] X. Wu, H. Li, L. Liu, and L. Xu, "Unidirectional single-frequency lasing from a ring-spiral coupled microcavity laser," *Appl. Phys. Lett.*, vol. 93, Aug. 2008, Art. no. 081105.

[30] X. Tu, X. Wu, M. Li, L. Liu, and L. Xu, "Ultraviolet single-frequency coupled optofluidic ring resonator dye laser," *Opt. Express*, vol. 20, pp. 19996–20001, Aug. 2012.

[31] Z. Li, Z. Zhang, T. Emery, A. Scherer, and D. Psaltis, "Single mode optofluidic distributed feedback dye laser," *Opt. Express*, vol. 14, pp. 696–701, Jan. 2006.

[32] W. Song, A. E. Vasdekis, Z. Li, and D. Psaltis, "Optofluidic evanescent dye laser based on a distributed feedback circular grating," *Appl. Phys. Lett.*, vol. 94, Apr. 2009, Art. no. 161110.
[33] Z. Li, Z. Zhang, A. Scherer, and D. Psaltis, "Mechanically tunable optofluidic distributed feedback dye laser," *Opt. Express*, vol. 14, Oct. 2006, Art. no. 10494.
[34] M. Gersborg-Hansen and A. Kristensen, "Optofluidic third order distributed feedback dye laser," *Appl. Phys. Lett.*, vol. 89, Sep. 2006, Art. no. 103518.
[35] M. Gersborg-Hansen and A. Kristensen, "Tunability of optofluidic distributed feedback dye lasers," *Opt. Express*, vol. 15, pp. 137–142, Jan. 2007.
[36] W. Song, A. E. Vasdekis, Z. Li, and D. Psaltis, "Low-order distributed feedback optofluidic dye laser with reduced threshold," *Appl. Phys. Lett.*, vol. 94, Feb. 2009, Art. no. 051117.
[37] S. Balslev and A. Kristensen, "Microfluidic single-mode laser using high-order Bragg grating and antiguiding segments," *Opt. Express*, vol. 13, pp. 344–351, Jan. 2005.
[38] X. Wu *et al.*, "Optofluidic laser for dual-mode sensitive biomolecular detection with a large dynamic range," *Nature Commun.*, vol. 5, Apr. 2014, Art. no. 3779.
[39] N. Zhang *et al.*, "Azimuthally polarized radial emission from a quantum dot fiber laser," *ACS Photon.*, vol. 3, pp. 2275–2279, Dec. 2016.

Chao-Yang Gong received the B.S. degree from the Wuhan University of Technology, Wuhan, China, in 2013. He is currently working toward the Ph.D. degree in optics in the University of Electronic Science and Technology of China, Chengdu, China. His research interest is focused on the optofluidic lasers for biochemical detection.

Yuan Gong received the Ph.D. degree in optics from the Institute of Optics and Electronics, Chinese Academy of Sciences, Chengdu, China, in 2008. He was a Lecturer in July 2008 in the University of Electronic Science and Technology of China, Chengdu, China, and has been an Associate Professor since 2011 in the same university. He was a visiting scholar in the University of Michigan, Ann Arbor, MI, USA, from January 2015 to January 2016. He has coauthored more than 100 peer-reviewed journal and conference papers and held more than 20 U.S./Chinese patents. His research interests include optical fiber sensors, optofluidic lasers, and biochemical detection.

Wei-Li Zhang received the Ph.D. degree in communication engineering from Southwest Jiaotong University, Chengdu, China, in 2008. From September 2008 to October 2010, he was a Research Fellow in the School of Electrical and Electronic Engineering, Nanyang Technological University, Singapore. He has been with the University of Electronic Science and Technology of China as an Associated Professor since November 2010 and was promoted to Professor in 2016. His research interests include optical fiber lasers, semiconductor microcavity lasers, and surface-plasmon physics.

Yu Wu received the B.Sc. degree from the University of Electronic Science and Technology of China, Chengdu, China, in 2003, and the Ph.D. degree in measurement technology and instruments from the Zhejiang University, Zhejiang, China, in 2008. He is currently an Associate Professor in the Key Lab of Optical Fiber Sensing and Communications (Education Ministry of China), University of Electronic Science and Technology of China. His research interests include optical fiber sensors, 2-D materials, and photonic devices.

Yun-Jiang Rao (M'11–SM'15–F'17) received the Ph.D. degree in optoelectronic engineering from Chongqing University, Chongqing, China, in 1990. He joined the Electric and Electronic Engineering Department, Strathclyde University, U.K., as a Postdoctoral Research Fellow during 1991–1992 and then the Applied Optics Group of the Physics Department, Kent University, U.K., as a Research Fellow, and then as a Senior Research Fellow during 1992–1999. His research interests include optical fiber sensors and lasers. From 1999 to 2004, he was a Chang-Jiang Chair Professor in Chongqing University. From 2004, he held the Chang-Jiang Chair Professor in University of Electronic Science and Technology of China. He is currently the Director of the Key Lab of Optical Fiber Sensing and Communications (Ministry of Education), University of Electronic Science and Technology of China. He is a Fellow of OSA and SPIE.

Gang-Ding Peng received the B.Sc. degree in physics from Fudan University, Shanghai, China, in 1982 and the M.Sc. degree in applied physics and the Ph.D. degree in electronic engineering from Shanghai Jiao Tong University, Shanghai, China, in 1984 and 1987, respectively. From 1987 to 1988, he was a Lecturer in Jiao Tong University. He was a Postdoctoral Research Fellow in the Optical Sciences Centre, Australian National University, Canberra, Australia, from 1988 to 1991. He has been with the University of New South Wales, Sydney, Australia, since 1991, was a Queen Elizabeth II Fellow from 1992 to 1996, and is currently a Professor in the same university. He is a Fellow of OSA and SPIE. His research interests include optical fibers, devices, and fiber sensors.

Xudong Fan received the B.S. and M.S. degrees from Peking University, Beijing, China, in 1991 and 1994, respectively, and the Ph.D. degree in physics and optics from Oregon Center for Optics, University of Oregon, Eugene, OR, USA, in 2000. Between 2000 and 2004, he was a project leader at 3M Company on fiber optics and photonic sensing devices for biomedical applications. In August 2004, he joined the Department of Biological Engineering, University of Missouri, as an Assistant Professor and was early-promoted to Associate Professor in 2009. In January 2010, he joined the Biomedical Engineering Department, University of Michigan. In 2014, he is early-promoted to Professor. His research includes photonic bio/chemical sensors, micro/nanofluidics, and nanophotonics for disease diagnostics and bio/chemical molecule analysis. He was an Associate Editor of *Optics Express*, and serves as member of the Editorial Board for Lab on a Chip. He is a Fellow of OSA, SPIE, and the Royal Society of Chemistry.